# Complete and deterministic discrimination of polarization Bell states assisted by momentum entanglement

M. Barbieri,[1,*,†] G. Vallone,[1,2,*] P. Mataloni,[1,*] and F. De Martini[1,*]

[1]*Dipartimento di Fisica dell'Universitá "La Sapienza" and Consorzio Nazionale Interuniversitario per le Scienze Fisiche della Materia, Roma, 00185 Italy*

[2]*Dipartimento di Fisica Teorica dell'Università di Torino and INFN-sezione di Torino-10100 Italy*

(Received 11 July 2006; published 17 April 2007)

A complete and deterministic Bell state measurement was realized by a simple linear optics experimental scheme which adopts two-photon polarization-momentum hyperentanglement. The scheme, which is based on the discrimination among the single photon Bell states of the hyperentangled state, requires the adoption of standard single photon detectors. The four polarization Bell states have been measured with average fidelity $F=0.889\pm0.010$ by using the linear momentum degree of freedom as the ancilla. The feasibility of the scheme has been characterized as a function of the purity of momentum entanglement.

DOI: 10.1103/PhysRevA.75.042317 PACS number(s): 03.67.Mn, 42.65.Lm, 03.67.Hk

In the domain of quantum information (QI) the completion of most fundamental quantum communication protocols involving bipartite entanglement, such as quantum teleportation [1], quantum dense coding [2], entanglement swapping [3], and some important quantum cryptographic schemes [4], requires the complete and deterministic identification of the Bell states which form the orthogonal basis for the reference Hilbert space of the bipartite system.

In quantum optics, pairs of correlated photons are generated by spontaneous parametric down conversion (SPDC) in a nonlinear (NL) optical crystal slab by choosing suitably phase matching conditions. Photon qubits can be encoded in several accessible degrees of freedom, such as polarization [5,6], linear and orbital momentum [7,8], and energy-time [9,10]. In particular, the four orthogonal entangled Bell states, expressed in the logic basis $|0\rangle$, $|1\rangle$:

$$|\Phi^{\pm}\rangle=\frac{1}{\sqrt{2}}(|0\rangle_A|0\rangle_B\pm|1\rangle_A|1\rangle_B),$$

$$|\Psi^{\pm}\rangle=\frac{1}{\sqrt{2}}(|0\rangle_A|1\rangle_B\pm|1\rangle_A|0\rangle_B) \quad (1)$$

form the complete maximally entangled basis of the Hilbert space $\mathcal{H}_A\otimes\mathcal{H}_B$ with $\dim(\mathcal{H}_A)=\dim(\mathcal{H}_B)=2$. In the particular case of a photon polarization entangled state, $|0\rangle$ and $|1\rangle$ correspond to the horizontal ($|H\rangle$) and vertical ($|V\rangle$) polarization states.

By standard linear methods, the discrimination of polarization Bell states cannot be achieved by simply performing a single joint measurement on the two particles. Indeed, a reliable experimental linear optical scheme capable to deterministically distinguish among the four entangled Bell states with 100% efficiency by using $2\times2$ entangled photon pairs does not exist and only a partial Bell state analysis with a maximum attainable value of 50% efficiency can be performed [11]. Recently, probabilistic complete Bell state analyzers for photonic quantum bits were demonstrated by using a controlled-NOT (CNOT) gate for photonic qubits [12].

The strategy adopted to overcome the intrinsic probabilistic character of any Bell analysis exploits further degrees of freedom to assist the measurement. In fact, by two photons entangled in $N>1$ degrees of freedom, namely, giving rise to an hyperentangled states spanning the $2^N\times2^N$ Hilbert space, a complete and deterministic Bell state analysis can be performed with standard linear optics [13,14]. In the case of double entangled states ($N=2$) it was shown that this operation can occur together with a CNOT logic operation between the control and target degrees of freedom [14]. An experimental demonstration of a complete analysis of the four polarization entangled Bell states has been recently given by Schuck *et al.* [15], who discriminate the polarization entanglement of two photons generated by a type-II NL crystal assisted by the intrinsic time-energy entanglement occurring in the SPDC process. The measurement apparatus described in that work consisted of a sequence of three different steps which allowed to distinguish among the four polarization entangled states. By that scheme, a full deterministic analysis of all the photon pairs requires the adoption of photon number resolving detectors.

In this paper we demonstrate that a complete and deterministic polarization ($\pi$) Bell state analysis can be performed by using the further degree of freedom of linear momentum ($\mathbf{k}$) as the ancilla. More precisely, the analysis of the Bell states (1) is carried out by discriminating among the single photon Bell states of a $\pi$-$\mathbf{k}$ hyperentangled two-photon state, at the Alice ($A$) and Bob ($B$) sites. By our scheme the four Bell states $|\Phi^+\rangle$, $|\Phi^-\rangle$, $|\Psi^+\rangle$, $|\Psi^-\rangle$, have been analyzed with high fidelity and equal detection probabilities by a single step measurement apparatus and using single photon detectors. For this purpose we used the SPDC source of $\pi$-$\mathbf{k}$ hyperentangled two-photon states, based on a single type-I $\beta$-$BaB_2O_4$ (BBO) crystal, already described in other experiments [see Fig. 1(a)] [16]. By this source we can generate over the whole BBO emission cone the polarization entangled states. By inserting a four-hole screen aligned to intercept the whole SPDC radiation, we select the photon pair passing through the modes $l_A-r_B$ (left Alice-right Bob)

---

*Web page URL http://quantumoptics.phys.uniroma1.it/

†Present address: School of Physical Sciences, the University of Queensland, 4072, Brisbane, QLD, Australia.

 

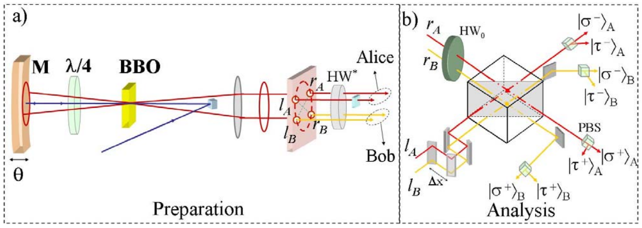


FIG. 1. (Color online) (a) Scheme of the hyperentanglement source: the polarization entangled state $|\Phi\rangle=\frac{1}{\sqrt{2}}(|H\rangle|H\rangle+e^{i\theta}|V\rangle|V\rangle)$ comes from the superposition of the degenerate cones of a type-I BBO crystal. The basic elements of the source are (i) a spherical mirror $M$, reflecting both the parametric radiation or the pump beam, whose micrometric displacement allows to control the state phase $\theta$ ($\theta=0,\pi$). (ii) A $\lambda/4$ waveplate, placed within the $M$-BBO path, which performs the $|H\rangle_A|H\rangle_B\rightarrow|V\rangle_A|V\rangle_B$ transformation on the two-photon state belonging to the left cone. (iii) A positive lens which transforms the conical parametric emission of the crystal into a cylindrical one. Mode selection is performed by a four hole mask. The $\lambda/2$ waveplate HW* intercepting modes $r_A, r_B$ performs the $|\Phi^{\pm}\rangle\rightarrow|\Psi^{\pm}\rangle$ transformation, the glass plate (on the $l_A$ mode) sets the phase of the momentum state. (b) Scheme of the Bell state analyzer (see text for details). The delay $\Delta x$ is simultaneously varied for both $l_A$ and $l_B$ modes.

or $r_A-l_B$, with coherent superposition between the two events. Then the hyperentangled states

$$|\Xi\rangle=|\mathrm{Bell}\rangle_{AB}\otimes|\psi^+\rangle=|\mathrm{Bell}\rangle_{AB}\otimes\frac{1}{\sqrt{2}}(|l\rangle_A|r\rangle_B+|r\rangle_A|l\rangle_B) \tag{2}$$

can be generated [16]. Here the state $|\mathrm{Bell}\rangle_{AB}$ can be either one of the two-photon polarization Bell states $|\Phi^{\pm}\rangle=\frac{1}{\sqrt{2}}(|H\rangle_A|H\rangle_B\pm|V\rangle_A|V\rangle_B)$, $|\Psi^{\pm}\rangle=\frac{1}{\sqrt{2}}(|H\rangle_A|V\rangle_B\pm|V\rangle_A|H\rangle_B)$.

The parametric source, which allows to finely control the phase of the $\pi$ states, generates the hyperentangled states $|\Phi^{\pm}\rangle\otimes|\psi^+\rangle$ [6]. The insertion of a zero-order $\lambda/2$ waveplate (WP) intercepting the modes $r_A$, $r_B$ [HW* in Fig. 1(a)] allows one to transform the state $|\Phi^+\rangle\otimes|\psi^+\rangle$ in $|\Psi^+\rangle\otimes|\psi^+\rangle$, while the transformation $|\Phi^-\rangle\rightarrow|\Psi^-\rangle$ is accompanied by a $\pi$ phase shift on the momentum entangled state $|\psi^+\rangle\rightarrow|\psi^-\rangle$. As a consequence, in order to generate $|\Psi^-\rangle\otimes|\psi^+\rangle$, we need to compensate this phase shift by suitable tilting of a thin glass plate inserted on mode $l_A$ [Fig. 1(a)]. The nonlocal character of the states $|\Xi\rangle$ was recently demonstrated by two different experiments, the all versus nothing test [17] and the Bell's inequalities violation of local realism with two degrees of freedom [18].

By the present method, we are able to discriminate among the four possibility $|\Phi^+\rangle$, $|\Phi^-\rangle$, $|\Psi^+\rangle$, $|\Psi^-\rangle$, by using the single photon Bell basis

$$|\sigma^{\pm}\rangle_i=\frac{1}{\sqrt{2}}[|H\rangle|l\rangle_i\pm|V\rangle|r\rangle_i],$$

$$|\tau^{\pm}\rangle_i=\frac{1}{\sqrt{2}}[|V\rangle|l\rangle_i\pm|H\rangle|r\rangle_i],\quad i=A,B \tag{3}$$

which allows one to express the four possible states $|\Xi\rangle$ as

$$|\Phi^{\pm}\rangle\otimes|\psi^+\rangle=\frac{1}{2}[\pm|\sigma^+\rangle_A|\tau^{\pm}\rangle_B\mp|\sigma^-\rangle_A|\tau^{\mp}\rangle_B+|\tau^+\rangle_A|\sigma^{\pm}\rangle_B$$
$$-|\tau^-\rangle_A|\sigma^{\mp}\rangle_B],$$

$$|\Psi^{\pm}\rangle\otimes|\psi^+\rangle=\frac{1}{2}[\pm|\sigma^+\rangle_A|\sigma^{\pm}\rangle_B\mp|\sigma^-\rangle_A|\sigma^{\mp}\rangle_B+|\tau^+\rangle_A|\tau^{\pm}\rangle_B$$
$$-|\tau^-\rangle_A|\tau^{\mp}\rangle_B]. \tag{4}$$

Each product state on the right-hand side identifies unambiguously one of the states $|\Xi\rangle$. Our scheme adopts linear momentum entanglement as the ancilla and polarization entanglement as the target. It is equivalent to the one proposed by Walborn *et al.* [14], except for the change of roles between the momentum and polarization degrees of freedom in that case. It is worth noting that by our scheme we distinguish among the four hyperentangled states $|\Xi\rangle=|\mathrm{Bell}\rangle_{AB}\otimes|\psi^+\rangle$. However, since the momentum state $|\psi^+\rangle$ is fixed, this is equivalent to distinguish among the four Bell polarization states.

Concerning the measurement apparatus, the two couples $l_A-r_B$ and $r_A-l_B$ are spatially and temporally combined onto a 50% beam splitter (BS) by an interferometric apparatus, where a trombone mirror assembly with fine delay adjustment $\Delta x$ is mounted on the left ($l$) modes. We set the position $\Delta x=0$ in correspondence of the superposition between the mode pairs $l_A-r_B$ and $r_A-l_B$, i.e., when the right ($r$) and left ($l$) optical paths of the interferometer are equal [16]. The analyzing apparatus is given by the BS which follows a 45° oriented $\lambda/2$ WP ($\mathrm{HW}_0$), inserted on the right ($r$) side in order to intercept both the Alice and Bob modes [Fig. 1(b)] [19].

We are then able to completely distinguish among the states (3), that are transformed by $\mathrm{HW}_0$ as

$$|\sigma^{\pm}\rangle_i\xrightarrow{\mathrm{HW}_0}|H\rangle\otimes\frac{1}{\sqrt{2}}[|l\rangle_i\pm|r\rangle_i],$$

$$|\tau^{\pm}\rangle_i\xrightarrow{\mathrm{HW}_0}|V\rangle\otimes\frac{1}{\sqrt{2}}[|l\rangle_i\pm|r\rangle_i],\quad i=A,B. \tag{5}$$

The BS discriminates between $|l\rangle_A+|r\rangle_A$ and $|l\rangle_A-|r\rangle_A$, $|l\rangle_B+|r\rangle_B$ and $|l\rangle_B-|r\rangle_B$, and polarization analysis on each BS output mode, performed by a polarizing beamsplitter (PBS), completes the single photon Bell state measurement [19]. Note that a completely deterministic Bell state analysis requires to detect the eight possible outputs of the apparatus [Fig. 1(b)]. In our proof of principle experiment we used four avalanche single photon detectors (Perkin Elmer SPCM-AQR14) on the transmitted modes of the PBS's. In the actual case the transmitted polarization is set by a further $\lambda/2$ WP before each PBS.

We can also explain in a different way this effect: the hyperentangled states (2) can be viewed as a three qubit states

$$|\Xi\rangle=|\mathrm{Bell}\rangle_{AB}\otimes\frac{1}{\sqrt{2}}(|0\rangle_C+|1\rangle_C), \tag{6}$$

where now the qubit $C$ is represented by the *couple of photons* in the coherent superposition of the two states $|0\rangle_C = |l\rangle_A |r\rangle_B$ and $|1\rangle_C = |r\rangle_A |l\rangle_B$. We are then able to completely discriminate between the four polarization Bell states $|\mathrm{Bell}\rangle_{AB}$ of the two qubits $A$ and $B$ with the *a priori* information about the state of the ancillary qubit $C$. This is the minimum *a priori* information (one over three qubits) required to perform a complete and deterministic Bell state analysis by linear optics. It is well known that this discrimination is not possible with only two qubits and no extra information [11]. Our approach improves the "standard" Bell state analysis where two bits of information are contained in the four Bell states and just one bit, concerning the information on which of the two kinds of states $|\Phi\rangle^{\pm}$ or $|\Psi\rangle^{\pm}$ the input particles are in, can be deterministically and completely extracted. It is worth noting the relevance for communication or cryptographic protocols of our method which allows to extract all (i.e., two) the bits of information that can be encoded in the states (6) [23].

Hence, Bell state analysis is performed by the following procedure.

(1) The phase information (the + or − signs) of the Bell states is transferred into the qubit $C$. In fact the $\mathrm{HW}_0$ operates in the following way:

$$|\Phi^{\pm}\rangle_{AB} \otimes |+\rangle_C \xrightarrow{\mathrm{HW}_0} |\Psi^{\pm}\rangle_{AB} \otimes |\pm\rangle_C,$$

$$|\Psi^{\pm}\rangle_{AB} \otimes |+\rangle_C \xrightarrow{\mathrm{HW}_0} |\Phi^{\pm}\rangle_{AB} \otimes |\pm\rangle_C,, \tag{7}$$

where $|\pm\rangle_C = \frac{1}{\sqrt{2}}(|0\rangle_C \pm |1\rangle_C)$.

(2) The BS discriminates between $|+\rangle_C$ and $|-\rangle_C$ as follows: the photons emerge either on the same or the opposite sides of the BS depending of the states $|+\rangle_C$ or $|-\rangle_C$, respectively.

(3) The four PBSs perform polarization analysis distinguishing between $|\Psi\rangle$ and $|\Phi\rangle$.

The four 3D histograms given in Fig. 2 show all the 16 possible combinations of the states (3) for either one of the input states $|\Phi^+\rangle$, $|\Phi^-\rangle$, $|\Psi^+\rangle$, $|\Psi^-\rangle$ and demonstrate the successful implementation of the Bell state analyzer. Each datum was obtained in an acquisition time of 10 s, while the typical count rate was $\simeq 1000\ \mathrm{s}^{-1}$ for each maximum measurement. The overall input-output histogram shown in Fig. 3 clearly indicates the high efficiency of the analysis performed by our scheme. The achieved fidelities of each Bell-state analysis are $F_{|\Phi^+\rangle} = 0.886 \pm 0.018$, $F_{|\Phi^-\rangle} = 0.895 \pm 0.018$, $F_{|\Psi^+\rangle} = 0.877 \pm 0.018$, $F_{|\Psi^-\rangle} = 0.899 \pm 0.018$, with an average value of $0.889 \pm 0.010$. Note that the adoption of the same measurement apparatus allows one to identify the four Bell states with almost the same fidelity. The noise contribution due to the unexpected coincidences is partially caused by the nonperfect purity of the polarization input state and partially due to imperfections of the analysis setup, e.g., mode mismatch on BS.

To test the feasibility of the Bell state analyzer realized by our scheme, we measured the output of the analyzer when the state $|\Psi^+\rangle$ is injected, while introducing noise in a controlled way in the ancilla state $|\psi^+\rangle$. This was performed by varying the value of $\Delta x$ in the interferometric apparatus. This procedure makes the two events, corresponding to the photons passing through the modes $l_A - r_B$ or $r_A - l_B$, more distinguishable and simulates an increasing amount of decoherence between the two possible mode pairs (not between one photon and the other). As a consequence the final state is

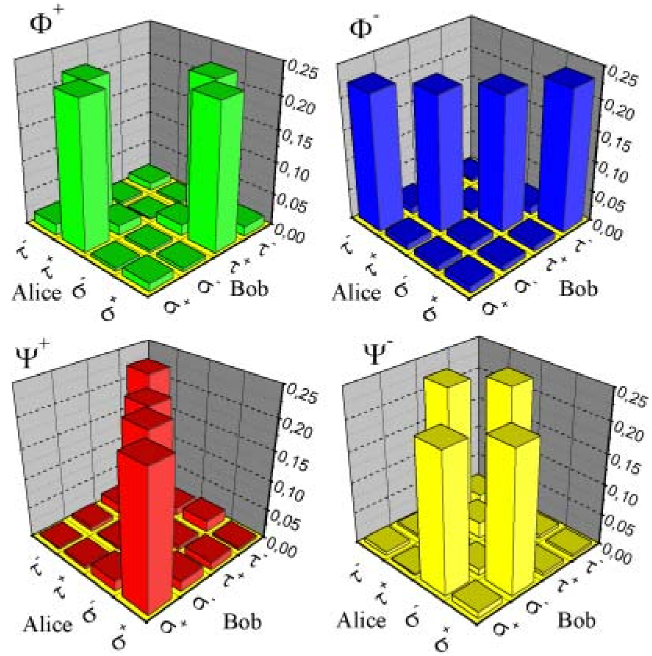


FIG. 2. (Color online) Experimental coincidence frequencies showing the complete Bell state analysis of the polarization states $|\Phi^+\rangle$, $|\Phi^-\rangle$, $|\Psi^+\rangle$, $|\Psi^-\rangle$. Relative errors are typically 2% for the maxima and 5% for the other terms.

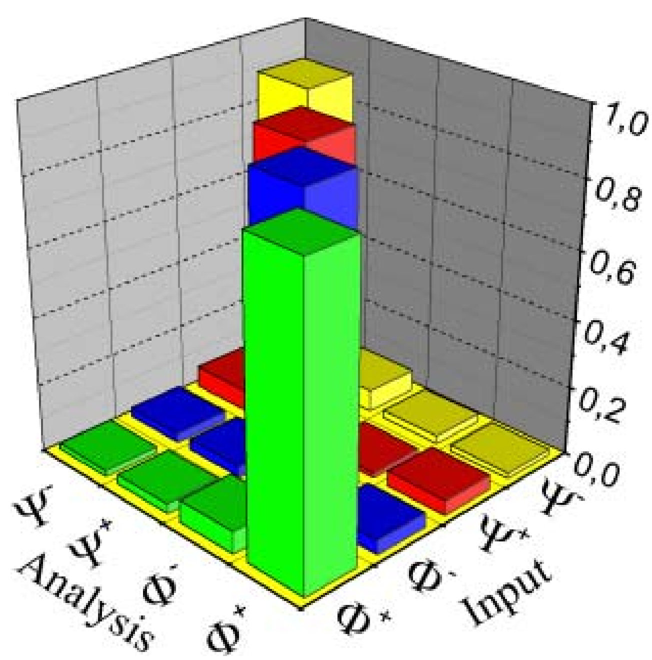


FIG. 3. (Color online) Overall experimental fidelities obtained by the Bell state analyzer for each input Bell state. Relative errors are typically 2% for the maxima and 5% for the other terms.

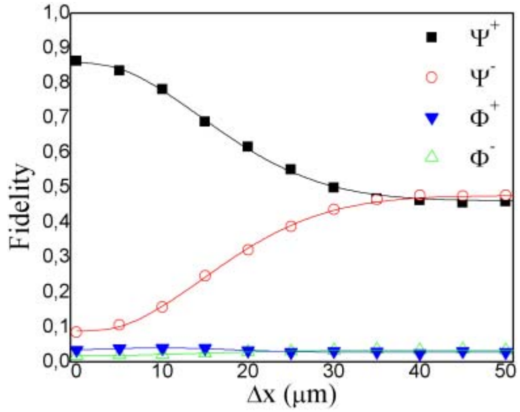


FIG. 4. (Color online) Output fidelities of the states $|\Phi^+\rangle$, $|\Phi^-\rangle$, $|\Psi^+\rangle$, $|\Psi^-\rangle$, vs the path length difference $\Delta x$ in the interferometric apparatus (input state, $|\Psi^+\rangle$). Error bars are smaller than the corresponding experimental points.

pure in polarization and mixed in the momentum degree of freedom. The experimental output fidelities, shown in Fig. 4, indicate, as expected, that $|\Psi^+\rangle$ and $|\Psi^-\rangle$ cannot be discriminated when $\Delta x > l_{\rm coh}$, the coherence length of the down converted photons imposed by the $\Delta\lambda=6$ nm interference filters before the detectors. The results of Fig. 4 demonstrate that a still efficient Bell state analysis, with $F_{|\Psi^+\rangle} \geqslant 0.75$, may be performed even with a partially degraded ancilla state. Similar results are expected when the input polarization entangled state is partially mixed.

We have presented in this paper a linear optical scheme based on two photon hyperentanglement which allows us to perform in a deterministic way the simultaneous measurement of the four polarization Bell states by using standard single photon detectors. By virtue of the simplicity of the measurement procedure and of the high fidelity experimentally attained, the present Bell state analyzer [Fig. 1(b)] may be applied to any source able to produce polarization-momentum entangled photons [5,16,20] and could be useful for the realization of QI protocols, in particular dense coding and quantum key distribution. Precisely, the implementation of cryptographic schemes with qudits up to $d=4$ (ququarts) requiring five mutually unbiased bases and the consequent Bell state measurement can be efficiently performed by adopting the method described in the present work [21]. Indeed, it has been shown that these systems are more robust against specific classes of eavesdropping attacks [22].

Thanks are due to Serge Massar for useful discussions. This work was supported by the FIRB 2001 (*Realization of Quantum Teleportation and Quantum Cloning by the Optical Parametric Squeezing Process*) and PRIN 2005 (*New Perspectives in Entanglement and Hyper-entanglement Generation and Manipulation*) of MIUR (Italy).


[1] C. H. Bennett, G. Brassard, C. Crepeau, R. Jozsa, and W. K. Wootters, Phys. Rev. Lett. **70**, 1895 (1993).

[2] C. H. Bennett and S. J. Wiesner, Phys. Rev. Lett. **69**, 2881 (1992).

[3] T. Jennewein, G. Weihs, J. W. Pan, and A. Zeilinger, Phys. Rev. Lett. **88**, 017903 (2002); F. Sciarrino, E. Lombardi, G. Milani, and F. De Martini, Phys. Rev. A **66**, 024309 (2002).

[4] A. Ekert, Nature (London) **358**, 14 (1992); N. Gisin, G. Ribordy, W. Tittel, and H. Zbinden, Rev. Mod. Phys. **74**, 145 (2002).

[5] P. G. Kwiat, K. Mattle, H. Weinfurter, A. Zeilinger, A. V. Sergienko, and Y. Shih, Phys. Rev. Lett. **75**, 4337 (1995); P. G. Kwiat, E. Waks, A. G. White, I. Appelbaum, and P. H. Eberhard, Phys. Rev. A **60**, R773 (1999).

[6] C. Cinelli, G. Di Nepi, F. De Martini, M. Barbieri, and P. Mataloni, Phys. Rev. A **70**, 022321 (2004).

[7] J. G. Rarity and P. R. Tapster, Phys. Rev. Lett. **64**, 2495 (1990).

[8] N. K. Langford, R. B. Dalton, M. D. Harvey, J. L. O'Brien, G. J. Pryde, A. Gilchrist, S. D. Bartlett, and A. G. White, Phys. Rev. Lett. **93**, 053601 (2004).

[9] J. D. Franson, Phys. Rev. Lett. **62**, 2205 (1989).

[10] J. Brendel, N. Gisin, W. Tittel, and H. Zbinden, Phys. Rev. Lett. **82**, 2594 (1999).

[11] N. Lütkenhaus, J. Calsamiglia, and K.-A. Suominen, Phys. Rev. A **59**, 3295 (1999); J. Calsamiglia and N. Lütkenhaus, Appl. Phys. B **72**, 67 (2001).

[12] J. L. O'Brien, G. J. Pryde, A. Gilchrist, D. F. V. James, N. K. Langford, T. C. Ralph, and A. G. White, Phys. Rev. Lett. **93**, 080502 (2004); Z. Zhao, A. N. Zhang, Y. A. Chen, H. Zhang, J. F. Du, T. Yang, and J. W. Pan, *ibid.* **94**, 030501 (2005); P. Walther and A. Zeilinger, Phys. Rev. A **72**, 010302(R) (2005).

[13] P. G. Kwiat and H. Weinfurter, Phys. Rev. A **58**, R2623 (1998).

[14] S. P. Walborn, S. Pàdua, and C. H. Monken, Phys. Rev. A **68**, 042313 (2003).

[15] C. Schuck, G. Huber, C. Kurtsiefer, and H. Weinfurter, Phys. Rev. Lett. **96**, 190501 (2006).

[16] M. Barbieri, C. Cinelli, P. Mataloni, and F. De Martini, Phys. Rev. A **72**, 052110 (2005).

[17] C. Cinelli, M. Barbieri, R. Perris, P. Mataloni, and F. De Martini, Phys. Rev. Lett. **95**, 240405 (2005).

[18] M. Barbieri, F. De Martini, P. Mataloni, G. Vallone, and A. Cabello, Phys. Rev. Lett. **97**, 140407 (2006).

[19] D. Boschi, S. Branca, F. De Martini, L. Hardy, and S. Popescu, Phys. Rev. Lett. **80**, 1121 (1998).

[20] T. Yang, Q. Zhang, J. Zhang, J. Yin, Z. Zhao, M. Zukowski, Z. B. Chen, and J. W. Pan, Phys. Rev. Lett. **95**, 240406 (2005).

[21] G. M. D'Ariano, P. Mataloni, and M. F. Sacchi, Phys. Rev. A **71**, 062337 (2005). G. Vallone, E. Pomarico, P. Mataloni, F. De Martini, and M. Barbieri, Phys. Rev. A (to be published)

[22] H. Bechmann-Pasquinucci and A. Peres, Phys. Rev. Lett. **85**, 3313 (2000).

[23] The present method is feasible only for quantum communication schemes, e.g., dense coding, which do not require independent photons.